Time-average velocity estimation through surface-wave analysis: Part 1-s-wave velocity

GEOPHYSICS, VOL. 82, NO. 3 (MAY-JUNE 2017); P. U49–U59, 13 FIGS.
10.1190/GEO2016-0367.1

Time-average velocity estimation through surface-wave analysis: Part 1 — S-wave velocity

Laura Valentina Socco[1], Cesare Comina[2], and Farbod Khosro Anjom[1]

ABSTRACT

In some areas, the estimation of static corrections for land seismic data is a critical step of the processing workflow. It often requires the execution of additional surveys and data analyses. Surface waves (SWs) in seismic records can be processed to extract local dispersion curves (DCs) that can be used to estimate near-surface S-wave velocity models. Here we focus on the direct estimation of time-average S-wave velocity models from SW DCs without the need to invert the data. Time-average velocity directly provides the value of one-way time, given a datum plan depth. The method requires the knowledge of one 1D S-wave velocity model along the seismic line, together with the relevant DC, to estimate a relationship between SW wavelength and investigation depth on the time-average velocity model. This wavelength/depth relationship is then used to estimate all the other time-average S-wave velocity models along the line directly from the DCs by means of a data transformation. This approach removes the need for extensive data inversion and provides a simple method suitable for industrial workflows. We tested the method on synthetic and field data and found that it is possible to retrieve the time-average velocity models with uncertainties less than 10% in sites with laterally varying velocities. The error on one-way times at various depths of the datum plan retrieved by the time-average velocity models is mostly less than 5 ms for synthetic and field data.

INTRODUCTION

Surface waves (SWs) in seismic records are traditionally considered noise to be filtered out during seismic processing. The potential of analyzing them to retrieve S-wave near-surface velocity models has been widely recognized in the scientific literature (Haney and Miller, 2013). SWs, commonly referred to as ground roll, can be analyzed using a processing workflow based on windowing and wavefield transforms to extract the local dispersion curves (DCs) (Socco et al., 2010). DCs express the relationship between the phase velocity and the frequency, and they depend on the velocity model along the propagation path. If the extraction of DCs is done such that each DC is representative of a small portion of the subsurface, the curve can then be inverted to provide a local 1D velocity model (Boiero and Socco, 2011; Strobbia et al., 2011). Due to its poor sensitivity to P-wave velocity, the DC is often inverted assuming an a priori value for Poisson's ratio (or V_P) and density, and only layer thickness and V_S are kept as inversion unknowns. The investigation depth depends on the propagating wavelengths, and it is therefore strongly data and site dependent. In general, the method is limited to near-surface layers ranging from some tenths to a few hundred meters of depth. The estimated near-surface velocity models can be used for several purposes, but one of the most important purpose in seismic exploration is the computation of S-wave long-wavelength static corrections (Al Dulaijan and Stewart, 2010; Roy et al., 2010; Douma and Haney, 2011; Boiero et al., 2013). Errors in long-wavelength statics significantly affect the quality of subsurface structural image. This is very relevant to imaging low-relief targets in zones with complex near-surface and low-velocity weathering layers (such as sand dunes), leading to long-wavelength statics with values greater than 80–90 ms (Ernst, 2007).

The nonuniqueness of the inversion is a well-known drawback of SW analysis (Socco et al., 2010), and it is very important to quantify the uncertainty that this process introduces to static computation. This is particularly critical when a large number of DCs are to be inverted using an automatic industrial workflow in which careful analysis of each DC by an expert operator is not feasible. The

First presented at the EAGE 77th Annual Conference and Exhibition. Manuscript received by the Editor 12 July 2016; revised manuscript received 19 November 2016; published online 21 March 2017.
[1]Politecnico di Torino, Torino, Italy. E-mail: valentina.socco@polito.it; farbod.khosroanjom@studenti.polito.it.
[2]Università di Torino, Torino, Italy. E-mail: cesare.comina@unito.it.

estimation of the static corrections requires that the time-average velocity at the depth of the (floating) datum plan is accurate enough to depict the lateral variability of the static shift along the line. The time-average velocity (V_z) at a given depth z allows the direct computation of the one-way time, and it can be defined as

$$V_z = \frac{\sum_n h_i}{\sum_n \frac{h_i}{V_i}}, \quad (1)$$

where n is the number of layers down to depth z and h_i and V_i are the thickness and the velocity of the ith layer, respectively. In the following, we will refer to the S-wave time-average velocity model as V_{Sz}.

Socco et al. (2015) and Mabyalaht (2015) addressed the effect of the nonuniqueness of the solution of SW inversion on the estimation of V_{Sz} using a Monte Carlo inversion algorithm. They showed that the nonuniqueness of the solution that affects the individual model parameters of a layered system, assumed as a reference model, collapses to very low values when the "acceptable" models are transformed into V_{Sz} profiles. Using synthetic and field data, they show that the uncertainty of V_{Sz} is in the range of 5% even when the velocity models are very challenging. This means that if the DC is used to estimate V_{Sz} instead of the layered velocity model, the solution nonuniqueness is not critical and the estimate is very robust.

The robustness of V_{Sz} estimation had also been investigated in the field of seismic hazard studies by Brown et al. (2000), Comina et al. (2011), and Aung and Leong (2015). They focused on the estimation of the $V_{S,30}$ (that is the V_{Sz} at 30 m depth) because this parameter is used to classify sites for seismic zonation. They showed that the estimate of $V_{S,30}$ through SW analysis is very robust. Moreover, they also show evidenced that the value of $V_{S,30}$ corresponds, with acceptable uncertainty, to the SW phase velocity at a certain wavelength (approximately equal to 36 m). This relationship suggests the existence of a strong link between the V_{Sz} at a certain depth and the phase velocity at a certain wavelength. In other words, a relationship exists between the investigation depth and the wavelength.

Other authors used relationships between the SW wavelength and the S-wave velocity model depth. Leong and Aung (2012) adopted a weighted average velocity method to relate V_{Sz} to the DC. Their approach is based on the evaluation of the contribution of the different layers to the propagating velocity at a certain wavelength. Weighting factors are determined for each propagating wavelength as a function of layer thicknesses. Haney and Tsai (2015) proposed a Dix-type relationship to obtain a depth profile directly from the DC. Their approach is based on the simplified assumption that each frequency component propagates in a homogeneous half-space and phase velocities are computed using a first-order approximation eigenfunction in the limit of a weakly heterogeneous velocity profile.

Socco et al. (2015) and Socco and Comina (2015) extended the concept of the wavelength/depth (W/D) relationship to the estimation of the V_{Sz} at any depth through a simple data transformation. They established a linear relationship between the wavelength of the DC and the depth of the V_{Sz} profile at which the S-wave velocity is equal to the phase velocity of Rayleigh waves. This relationship allows the DC to be directly transformed into a V_{Sz} model that provides the one-way time value at any depth within the investigation limit. Here, we further develop this concept by improving the W/D relationship estimation using a piecewise polynomial fitting. Socco et al. (2015) and Socco and Comina (2015) also used the W/D relationship estimated for one reference velocity profile to transform a set of synthetic DCs into the relevant V_{Sz} profiles with variable velocity. We investigate the statistical uncertainties of this approach and the effect of the selection of a specific reference velocity profile within the data set. Because the method is essentially a data transformation, it is of paramount importance to test its performance on real data. In this work, we provide two field cases with different data quality to assess the applicability of the method in laterally varying sites.

The paper is organized as follows: First, we outline the method using a single synthetic profile example. Then, we extend the estimation to a set of variable velocity models, and we show the effect of the selection of the reference DC. We show the results on two synthetic data sets, one with velocity always growing with depth and one including a velocity inversion. Finally, we apply the method to two field data sets.

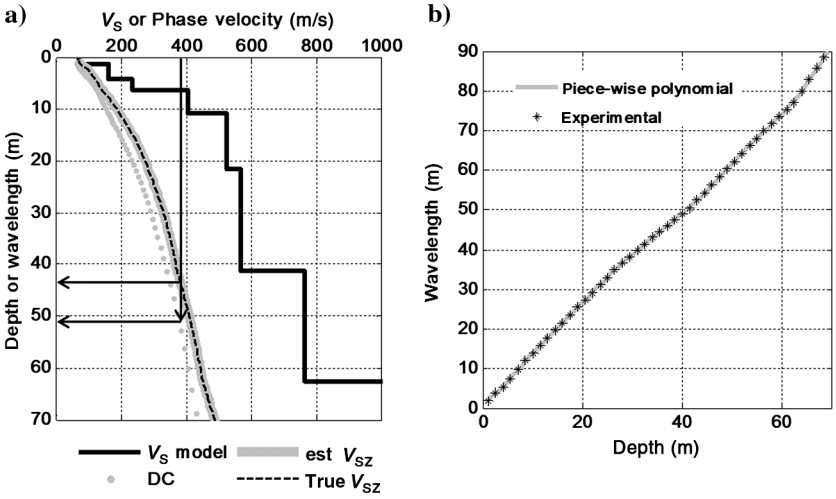

Figure 1. (a) The synthetic V_S model (solid black), the corresponding true V_{Sz} (dashed black), the Rayleigh-wave DC (gray dots), and the estimated V_{Sz} (solid gray); the vertical axis corresponds to depth for the V_S profiles and to wavelength for the DC, and the horizontal axis corresponds to V_S for the V_S profiles and to the SW phase velocity for the DC; (b) the W/D relationship (black asterisks) and the piecewise polynomial fit (solid gray).

METHOD

We use a 1D synthetic example to outline our method. We consider a synthetic 1D layered velocity model, its corresponding V_{Sz}, and the relevant fundamental mode DC as a function of wavelength (Figure 1a). In this paper, we always refer to the fundamental mode only; hence, for "dispersion curve," we intend "dispersion curve of the fundamental mode of Rayleigh waves." For each V_{Sz} value, we search for the wavelength at which the phase velocity of the DC is equal to the V_{Sz} (see the arrows in Figure 1a). We obtain a set of W/D pairs at which V_{Sz} and phase velocity are equal. The obtained W/D pairs are plotted in Figure 1b and interpolated with a piecewise polynomial fit. Using this polynomial relationship, it is now possible to directly retrieve the V_{Sz} from the DC (solid gray profile in Figure 1a) within the investigation limit. The use of a piecewise polynomial relationship instead of a

linear regression is thoroughly addressed by Khosro Anjom (2016), and it is discussed in the "Discussion" section.

The W/D relationship has a strong physical link with SW propagation: SWs propagate along the free surface over a cylindrical wavefront whose thickness depends on the wavelength. This feature creates the typical dispersive behavior of SWs in vertically heterogeneous media: The propagation velocity of each wavelength depends on the velocities (V_S) of the layers down to the wavefront thickness. This can be shown by computing the displacements induced by the propagation of SWs at different depths. In Figure 2, we show the normalized amplitude of vertical displacements at different depths for each propagating wavelength for the model of Figure 1a. In the same figure, we also report the W/D relationship estimated in Figure 1b. It can be noted that the W/D relationship roughly corresponds to the limit at which the displacements become negligible (10%). The vertical displacements are computed using the code implemented by Maraschini (2008) and based on the work of Herrmann and Ammon (2002), who use the method introduced by Thomson (1950) and Haskell (1953) and modified by Dunkin (1965).

To test the proposed method, we show that the same process can also be applied to a velocity model that is more challenging for SW analysis. In Figure 3, we show the same scheme presented in Figure 1 for a velocity profile that contains a low-velocity layer (LVL) embedded in higher velocity layers. The results confirm the applicability of the proposed procedure also in this case.

We have shown that if the W/D relationship is known, the V_{Sz} can be directly estimated from the DC. However, to estimate the W/D relationship, we need the V_{Sz}. Therefore, up to now, it seems that we are in sort of a loop. Hence, the question that arises is: How can we make this concept useful for exploration? In the following, we will show that, if a set of DCs corresponding to unknown highly variable velocity models is available, we can still estimate V_{Sz} of all the models by using the W/D relationship estimated only for one known model.

SYNTHETIC EXAMPLES

We created a set of 76 V_S models by randomly perturbing the velocities and thicknesses of the reference model in Figure 1. For all the models, we imposed a velocity growing with depth bounded by a constant velocity half-space. This synthetic data set is aimed at simulating a site with lateral variations in the overburden velocity and thicknesses. The lateral variability of the V_S is up to 150%, which corresponds to a variability of V_{Sz} of approximately 120%. In Figure 4, we show the V_S models and the relevant DCs, and we compare the true V_{Sz} with the V_{Sz} estimated by using the W/D relationship of Figure 1b. Hence, by knowing only one velocity model and having the DCs of all the others, we estimated the V_{Sz} of the whole data set. We show the distribution of the estimation error with depth in Figure 5a. It can be noticed that, apart from the very shallow depths, the error falls within 10%. Therefore, the estimation is able to reconstruct the lateral variability of V_{Sz} (120%) with acceptable accuracy by applying the W/D relationship estimated for one model to all the others.

Because we use one reference model to estimate all the others, it is important to investigate the effect of the choice of the reference model for the computation of the W/D relationship. Hence, we repeated the estimation performed for the model in Figure 1, using all the other models, one at a time. This implies the repeated calculation of a W/D relationship calibrated on the chosen reference model each time. In Figure 5b, we report a box plot of the mean V_{Sz} estimation error for the whole data set using different reference profiles for estimating all the others. The box plot is characterized by three lines that identify the lower quartile, the median, and the upper quartile values of the distributions, respectively; the whisker lines, extending from each end of the boxes for 1.5 times the corresponding interquartile distance, show the extent of the rest of the data. The crosses are outlier data with values beyond the ends of the whiskers.

The mean estimation error remains less than 10% independently from the chosen reference profile. In most cases, it is less than 5%. A few profiles (e.g., profile 31) give a slightly higher error. Never-

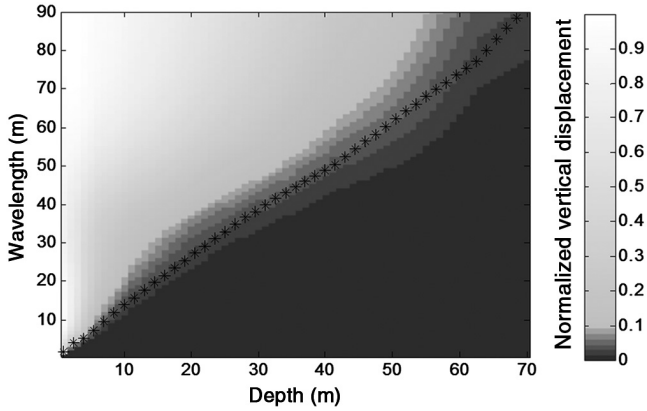

Figure 2. Normalized amplitude of vertical displacements as a function of depth and wavelength for SW propagation for the model from Figure 1a. The black asterisked line is the W/D relationship in Figure 1b.

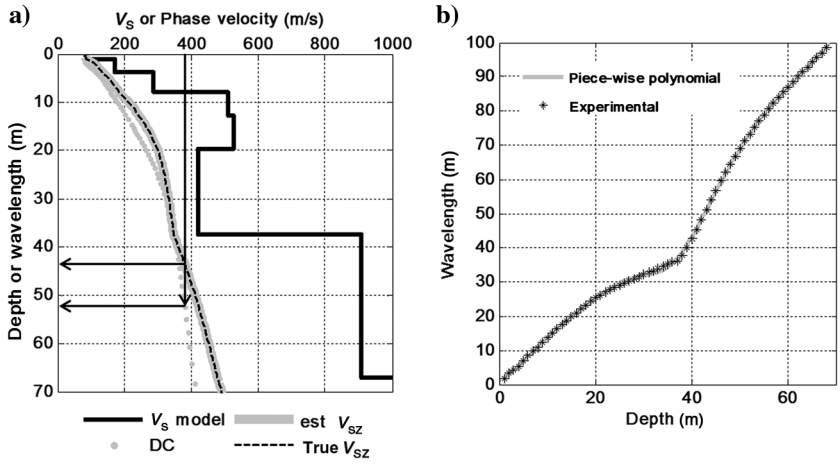

Figure 3. (a) The synthetic V_S model (solid black), the corresponding true V_{Sz} (dashed black), the Rayleigh-wave DC (gray dots), and the estimated V_{Sz} (solid gray); the vertical axis corresponds to depth for the V_S profiles and to wavelength for the DC, and the horizontal axis corresponds to V_S for the V_S profiles and to the SW phase velocity for the DC; (b) the W/D relationship (black asterisks) and the piecewise polynomial fit (solid gray).

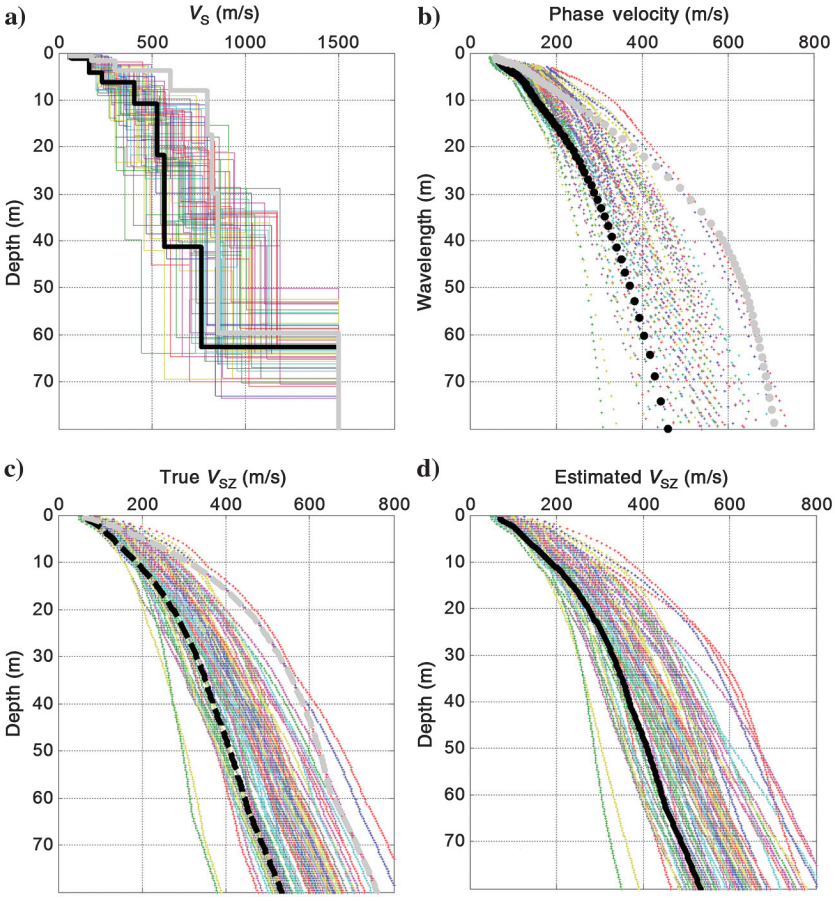

Figure 4. (a) Display of all synthetic models in relation to the reference profile (solid black) and critical profile 31 (solid gray); (b) DCs corresponding to the synthetic models the reference profile (black dots), and the critical profile 31 (gray dots) — all are plotted as a function of wavelength; and (c) true V_{SZ} for all the models in panel (a) and evidence of the reference one (dashed black) and critical profile 31 (dashed gray); V_{SZ} is estimated using the W/D relationship in Figure 1b for all models, including the reference model (solid black).

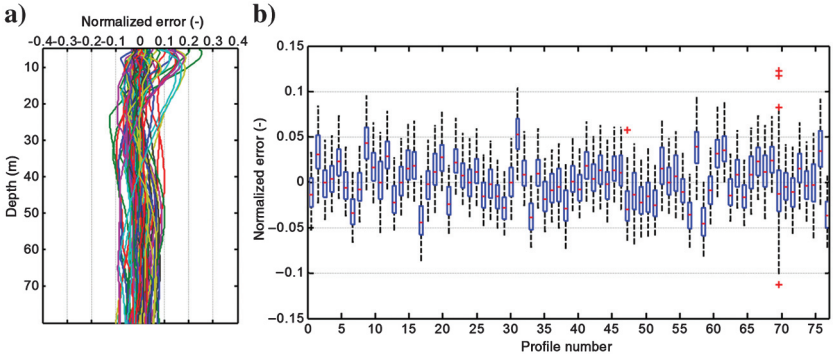

Figure 5. (a) Normalized estimation error of the V_{SZ} with depth for the data set using W/D relationship of Figure 1b; (b) box plot of the mean V_{SZ} estimation error for the whole data set using different reference profiles (and different W/D relationships) for estimating all the others. In the box plot, the three lines identify the lower quartile, the median, and the upper quartile values of the distributions, respectively; the whisker lines, extending from each end of the boxes for 1.5 times the corresponding interquartile distance, show the extent of the rest of the data; the crosses are outliers.

theless, these profiles have corresponding DCs that are out of trend with respect to the rest of the data set (see in Figure 4b, in which profile 31 is evidenced within the data set). The importance of the selection of the reference profile will be further discussed later.

The same assessment is made for a synthetic data set obtained from the velocity model with LVL (Figure 3). In Figures 6 and 7, we report the results similarly to Figures 4 and 5. The synthetic examples show that it is possible to directly estimate the V_{SZ} with error in the range of 12%, for a variable set of velocity models starting from one known V_{SZ} model and a set of DCs. The presence of an LVL within the data set only slightly increases the estimation error with respect to a site with a velocity always increasing with depth.

FIELD EXAMPLES

We used two vintage data sets for which V_S models had been estimated in previous works by inverting the experimental DCs (Socco et al., 2008, 2009). The two DC data sets are extracted from seismic records acquired for high-resolution seismic reflection surveys. The extraction of the DCs was performed in the f-k domain using a moving window that spanned the seismic line. As a result, a set of local DCs along the line is available in both cases. The two data sets have different data quality and model complexity. The first presents very slight lateral variations and a velocity model with a gradual velocity increase with depth. Moreover, the DCs are very smooth and continuous with a high signal-to-noise ratio. The second data set is more challenging, and an LVL is known to be present from previous surveys. The data quality is also critical with noisy DCs presenting several gaps. In the following, we provide a brief description of the two data sets, we select reference models and we use them to estimate the W/D relationships that we then apply to the whole seismic lines. For the second data set, because the line crosses two different environments that present different velocities, the data set is divided in two sub-data sets and a reference model is selected for each of them. We show the results in terms of V_{SZ} models and compare them with the results obtained from previous inversions and borehole data. We use the results of DC inversion as a benchmark, being aware that the inversion results are nonunique and that they cannot be considered as the ground truth. Nevertheless, with DC inversion being an accepted method to retrieve S-wave near-surface velocity, we consider the comparison with inversion results meaningful for validating the proposed method. We also compare our results with borehole and DC inversion in terms of velocity models and one-way time values.

Field 1: La Salle

The site is located in the Alps, on the alluvial fan of La Salle (northwest Italy). The Quaternary deposit (sand and gravel, with pebbles and blocks) of the fan is 1.5 km long and almost 2.5 km wide with an expected maximum thickness of approximately 200 m. The deposit was the object of a geophysics campaign in 2007, and details about the site and the geophysical investigation can be found in Socco et al. (2008). Two orthogonal high-resolution P-wave seismic reflection lines with lengths of approximately 1 km were acquired, and, besides the seismic reflection processing, the data were also used to extract a set of SW DCs and to pick P-wave traveltimes. The DCs were inverted using a laterally constrained inversion (LCI) algorithm (Auken and Christiansen, 2004; Socco et al., 2009) and provided V_S sections down to a depth of 60 m. In five sites located along the two lines, additional SW data were acquired performing multichannel active SW acquisitions and passive noise measurements with 2D arrays. Five broadband DCs were obtained by merging active and passive data, and they were individually inverted using a Monte Carlo algorithm. These broadband DCs allowed V_S profiles down to a depth of 120 m to be obtained. Also, S-wave downhole tests (DHTs) were performed in two boreholes located in the vicinity of the seismic lines. Details about the processing and inversion are reported in Socco et al. (2008, 2009). Here, we focus on the DCs extracted along line 1. From previous results, we know that the site does not present significant lateral variability and that the S-wave velocity grows gradually with depth with a typical trend of gravel deposits.

In Figure 8a, we show the set of experimental DCs as a function of wavelength together with the reference model. The data quality is very good, and the curves are smooth and fairly similar to each other. The maximum wavelength considered is 60 m. The reference model is obtained by inverting one of the DCs from a site near the seismic line (site A in Socco et al., 2008) obtained by merging active and passive SW data. The inversion is performed using a Monte Carlo inversion (Socco and Boiero, 2008) in which the V_S and Poisson's ratio are free to vary in each layer. In Figure 8b, we show the W/D relationship for the reference model. We then use the relationship in Figure 8b to directly estimate V_{Sz} along the line.

In Figure 9, we report the obtained results in term of V_{Sz} models along the line, and we compare them with V_{Sz} computed from the results of the LCI of the whole data set (Socco et al., 2008). We consider the LCI results as our benchmark, and we compute the normalized difference of our direct estimation of V_{Sz} with respect to the LCI results (Figure 9c). In Figure 9c, we superimpose the data points of the experimental DCs as a function of wavelength. We also report the results of the DHT in terms of V_{Sz} using the same color scale used for the velocity sections and the normalized differ-

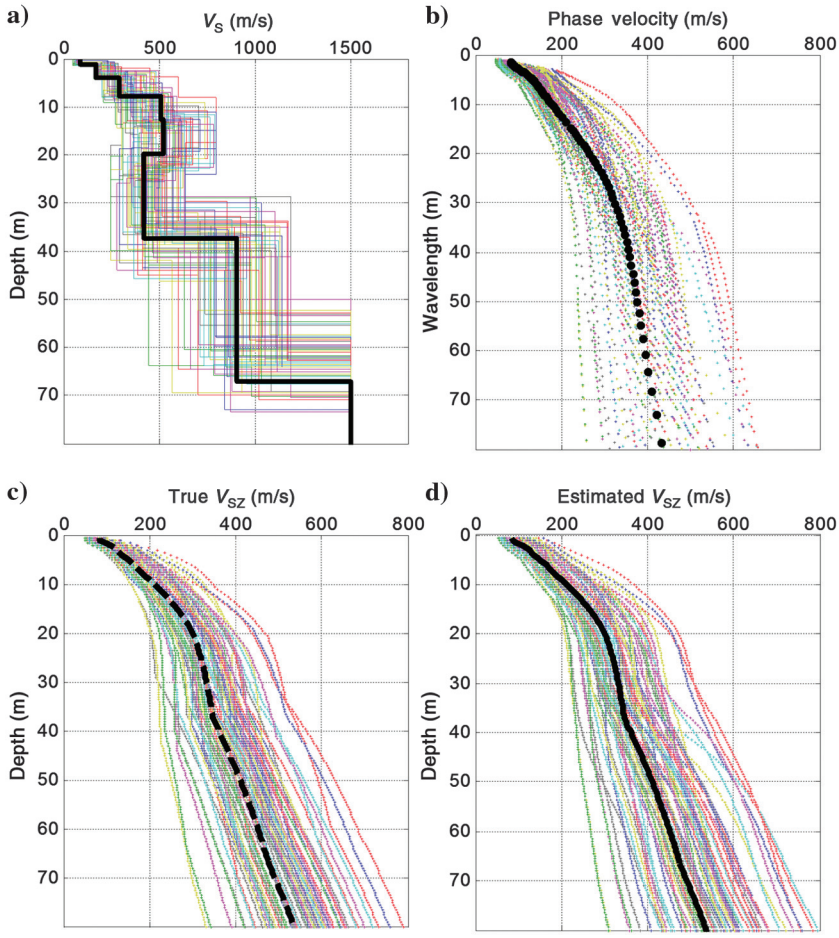

Figure 6. (a) Display of all the synthetic models in relation to the reference profile (solid black); (b) DCs corresponding to the synthetic models the reference profile (black dots) — all are plotted as a function of the wavelength; and (c) true V_{Sz} for all the models in panel (a) and evidence of the reference model (dashed black); V_{Sz} is estimated using the W/D relationship in Figure 3b for all models, including the reference model (solid black).

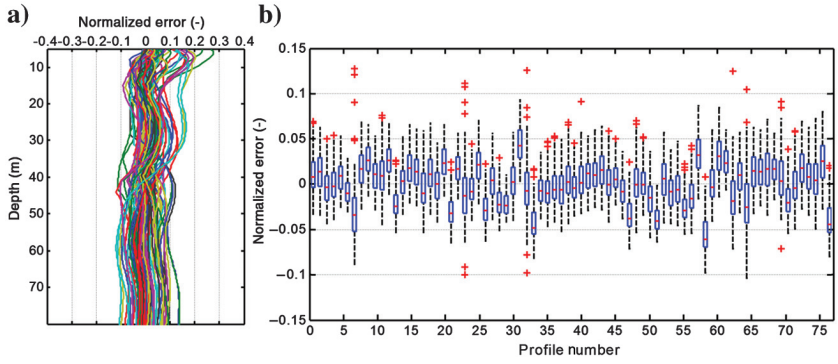

Figure 7. (a) Normalized estimation error of V_{Sz} with depth for the data set using the W/D relationship of Figure 3b; (b) box plot of the mean V_{Sz} estimation error for the whole data set using different reference profiles (and different W/D relationships).

Figure 8. Field case 1: (a) the DC data set (gray asterisks), the DC (black dots) of the reference model (solid black), and reference V_{Sz} (dashed black); (b) the W/D relationship for the reference model (black asterisks) and the piecewise polynomial fit (solid gray) used to estimate the V_{Sz} for the whole data set.

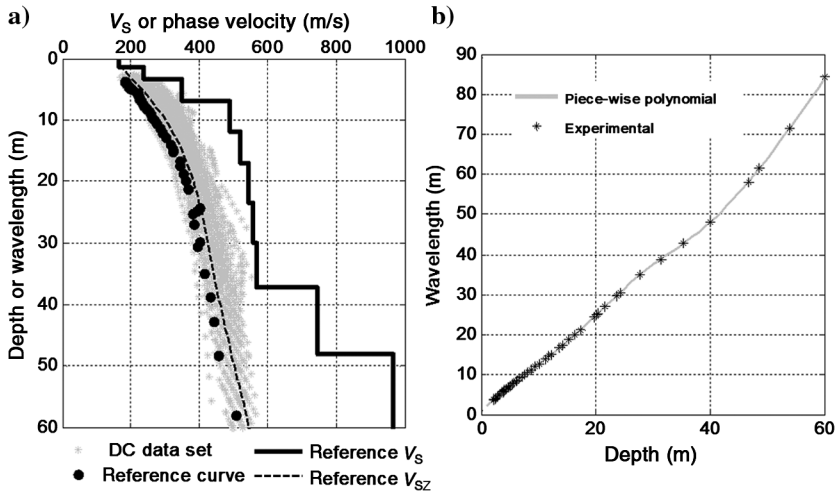

Figure 9. Field case 1: (a) V_{Sz} obtained from an LCI of all the DCs and DH results; (b) V_{Sz} estimated using the W/D piecewise polynomial fit relationship in Figure 8b, reference location for site A is also evidenced together with DH results; and (c) normalized difference between the two V_{Sz} models and DH results. The black crosses represent the DC data points of all the DCs plotted as a function of wavelength; and (d) one-way time along the line at a floating datum plan at depth of 55 m (reported in [a and b]) for inverted and approximated V_{Sz}.

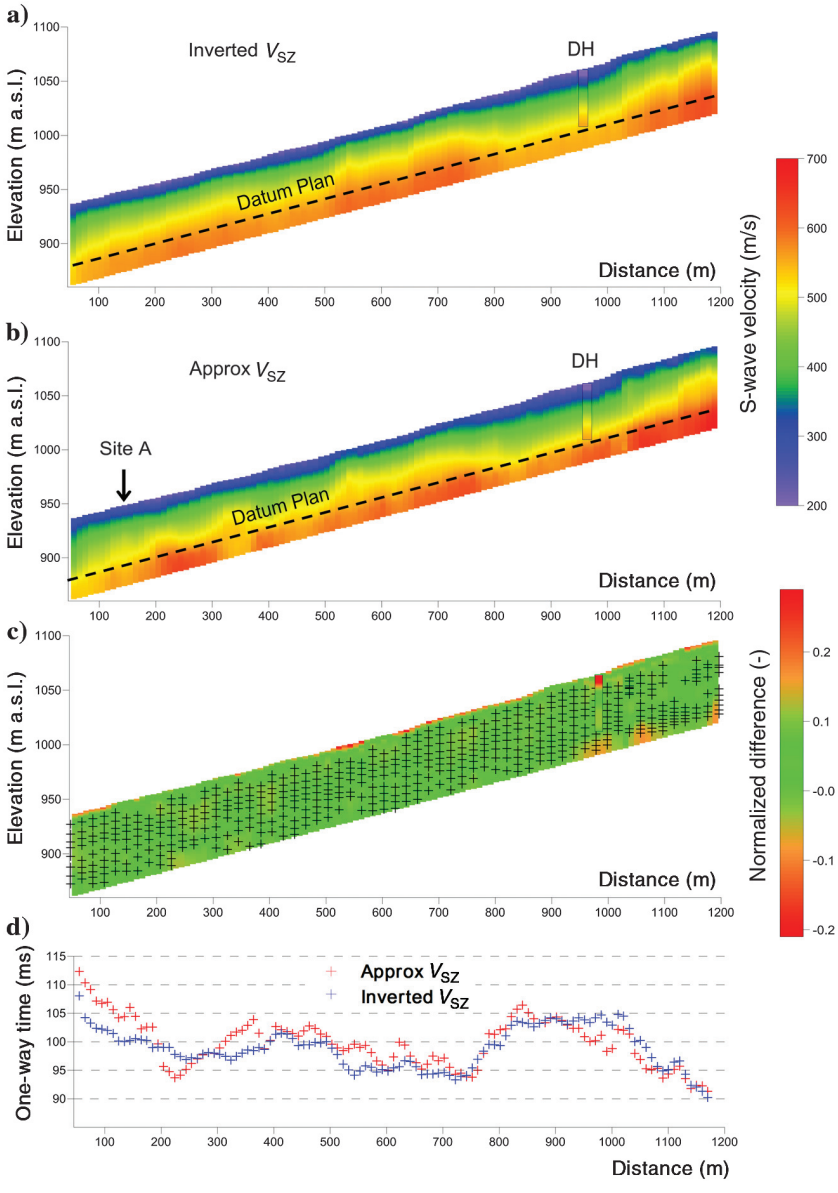

ence of our results with respect to the DHT. In Figure 9d, we report the one-way time (static shift) at a floating datum at a 55 m depth computed along the line using the LCI results and our approximated results.

Apart from very few zones within the section, the V_{Sz} is estimated with a mean difference with respect to inverted data of less than 5% along the whole line. The site presents a very slight lateral variability, which is very well reconstructed by the direct estimation (see the comparison between Figure 9a and 9b). The data are also in good agreement with the DHT except in the first 5 m, in which the DHT provides lower velocity than the LCI and our direct estimation. Nevertheless, this error is recovered below 5 m, where the difference remains in the range of 10% or lower. The static shifts computed at a depth of 55 m (below the top of the first high-velocity layer) show maximum difference of the order of 5 ms and provide very similar trends. The LCI results are slightly smoother, and this can be due to the use of lateral constraints among neighboring models during inversion.

Field 2: Torre Pellice

The site is located in an alpine valley in the town of Torre Pellice (northwest Italy). It presents a sequence characterized by the fringe of an alluvial fan with coarse and irregularly shaped sediments, fluvial sediments with variable thickness (10–50 m), lacustrine sediments, and the bedrock, which is expected at more than a 100 m depth in the central part of the valley. In 2007, a high-resolution reflection survey was performed along a 800 m line across the valley in the framework of a seismic hazard study (for details about data acquisition and processing, see Socco et al. [2009] and Boiero and Socco [2014]). Data from the seismic line were also used to extract a set of SW DCs and to pick P-wave traveltimes. The DCs were then inverted using a joint P- and S-wave inversion algorithm (Boiero and Socco, 2014), and they provided the V_S sections down to a depth of approximately 50 m. The seismic line crosses two different geologic environments: the zone close to the river (from zero to approximately 250 m) on the south, in which nine DCs are available, and the zone on the north that overlies an alluvial fan (from 250 m to the end of the line), in which 27 DCs are available. The maximum wavelength obtained ranges from 30 to 50 m in the south zone and from 60 to 100 m in the north zone. The minimum values of the wavelength are approximately 4 m, thus providing rough information on the uppermost layer.

On this data set, we performed the same analysis as for field case 1. However, the two sets of DCs present two different trends and well-sepa-

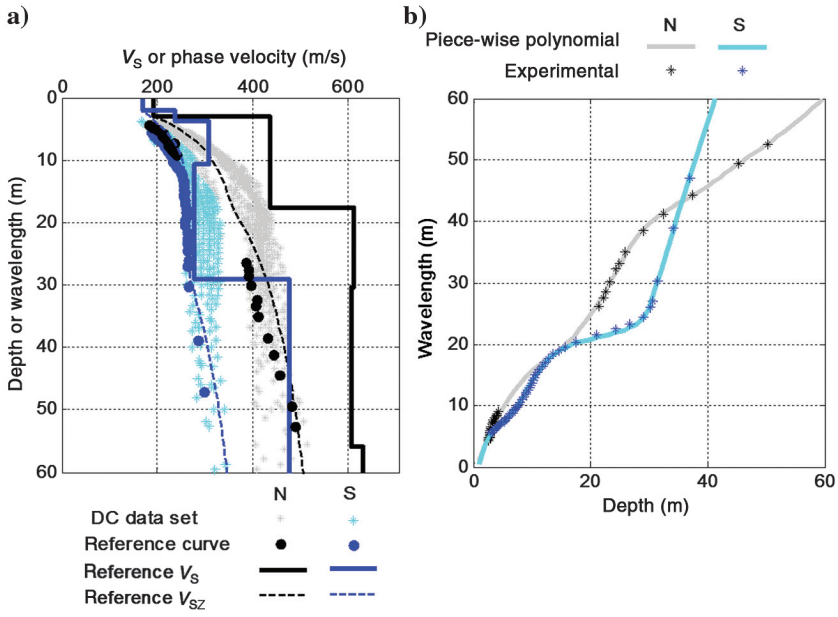

Figure 10. Field case 2: (a) the DC data set, the DC of the reference models, and reference V_{Sz}; (b) the W/D relationships for the reference models and piecewise polynomial fit used to estimate the V_{Sz} for the whole data set. The difference between the north and south zones is evident.

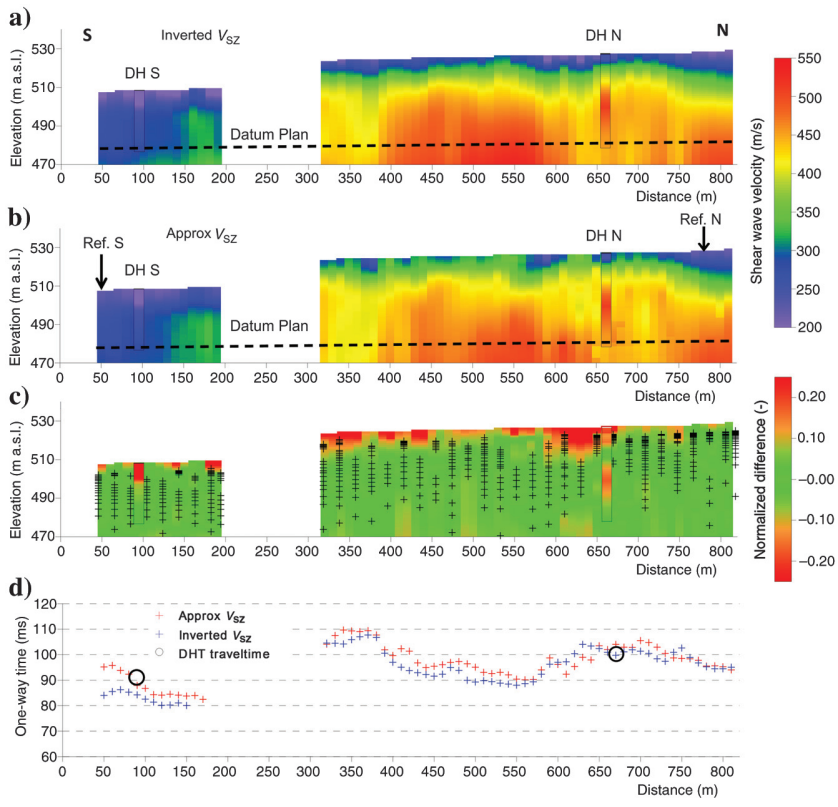

Figure 11. Field case 2: (a) V_{Sz} obtained from joint inversion of all the DCs and DH results; (b) V_{Sz} estimated using the W/D piecewise polynomial fit relationships in Figure 10b, and the reference locations are evident together with the DH results; (c) normalized difference between the two V_{Sz} models and DH results, and the crosses represent the DC data points of all the DCs plotted as a function of wavelength; and (d) one-way time along the line for the datum plan reported in panels (a and b) for inverted and approximated V_{Sz} and DHT traveltimes.

rated velocity ranges (lower in the south zone, see Figure 10a). It would then be inappropriate to use a single reference model to process the two sets together. Hence, we selected two reference models: one from the north zone and one from the south zone and two W/D relationships to be applied in the two zones. Both reference models are taken from the data set itself by selecting the models estimated through joint inversion with the broadest bandwidth DCs in the two zones.

In Figure 10, we show the DC data set, the reference models and the W/D relationships. It is worth noticing that for this data set, the quality of the DCs, and of the selected references is significantly worse than for the data set in field case 1. As a consequence, particularly for the north zone, the piecewise polynomial interpolation of the W/D pairs is based on few data points and interpolated within the frequency band that presents gaps in the experimental DC (Figure 10b). This field case is more challenging than field case 1, not only because the quality of the data is worse but also because this site presents a higher degree of lateral variability. Moreover, in some zones of the velocity model, we expect the presence of a velocity decrease due to soft lacustrine sediments below the stiffer fluvial sediments. This velocity decrease is very slight in the fourth layer of both of the chosen reference profiles (Figure 10a).

In Figure 11, we report the results in terms of V_{Sz} models along the line compared with the joint-inversion results and their normalized difference with the same scheme as Figure 9. Taking into account the aforementioned limitations of experimental data, the V_{Sz} is well-retrieved and lateral variations are reconstructed. The data quality affects the quality of the results, but most of the higher error zones (Figure 11c) are related to poor coverage, particularly in the lower portion of the section. The mean difference with respect to inverted data remains similar to the previous field case. Also, in this case, we report the DHT results and compare them with the data. The differences with respect to DHT result are greater than for site 1, and DHT in the north zone presents a higher variability of the velocity with depth than the velocity models obtained from the joint inversion and our direct estimation. Regarding the comparison with DHT, it is worth mentioning that the boreholes are located at a certain distance from the line, in particular, the one in the south zone is approximately 200 m far. We show the one-way time along the line for the datum plan indicated in Figure 11a and 11b (located at a depth of approximately 45 m in the north zone and 30 m in the south zone) computed from joint-inversion results and our direct estimation results. Also, in this case, the trends are in very good agreement and the difference is mostly within 5 ms. In Figure 11d, we also report the DHT traveltimes at the datum plan depth; it can be observed that in the south zone, the DHT traveltime is in better agreement with our estimation with respect to LCI data.

DISCUSSION

We developed and tested a method to directly transform surface-wave DCs into time-average velocity (V_{Sz}) models without the need of inverting the data. Given a data set of DCs along a seismic line and with the knowledge of only one V_S model corresponding to one of the DCs, we estimate the relationship between the DC wavelength and the depth (W/D) of the V_{Sz} profile and use it to predict all the V_{Sz} profiles corresponding to the other DCs. The W/D is estimated through a piecewise polynomial fit that provides a better estimate of the time-average velocity models than a linear fit. In particular, Khosro Anjom (2016) performed tests on linear versus piecewise polynomial fit on the same data sets used in this work. For the first synthetic data set, the global average error computed considering all the results reported in the box plot in Figure 5b was 3.45% for polynomial versus 3.55% for linear, whereas for the second synthetic data set, the errors were 4.9% and 6.8% for polynomial and linear fit, respectively. For data set of field case 2, the results have a global average error of 5.48% for the polynomial against an error of 14.97% for the linear fit. The piecewise polynomial fit is therefore to be considered more reliable than the linear fit in complex V_{Sz} models, and it is generally recommended. Conversely, for smooth velocity gradients, a linear fit also provides reliable results.

The reference model used to estimate the W/D relationship can be obtained by inverting one of the available DCs or from independently available information. Socco et al. (2015) and Mabyalaht (2015) have shown that the nonuniqueness of the SW inversion affects very slightly the estimate of time-average velocity, and hence, the V_{Sz} obtained from inverted profiles is very robust. Hence, the reference V_{Sz} can be reliably obtained through the inversion of one of the available curves if no a priori information is available.

In the synthetic data examples, we have used one of the models of the data set as a reference model; hence, the W/D relationship has been estimated without error (true V_S model and theoretical DC). In these conditions, we have shown that reliable V_{Sz}, with errors less than 10%, can also be estimated for sites with high lateral variability, in which the V_S varies among the models of more than 150% (see Figures 4a and 6a). Hence, in spite of estimating the W/D relationship for one model only, it can be used to predict the others picturing the lateral variability. Moreover, the quality of the estimate shows little dependence with the choice of the reference model in the data set. This is shown in the error box plots of Figures 5b and 7b.

Nevertheless, in the case of strong lateral variability, it might be wise to split the data set in subdata sets and process them separately, in fact, if a DC with a significantly different trend from the others is used to estimate the W/D relationship, this can introduce higher errors in the estimated V_{Sz}. As an example, curve number 31 in the first synthetic example (Figures 4a–4c and 5b) produces a worse estimate when used with its relevant model as a reference for W/D estimation. We have also shown on field case 2 that by plotting all the DCs together, it is easy to identify subsets of data to be processed separately. For each subset, the most representative curve in terms of the velocity range and frequency bandwidth is selected as a reference for the estimation of the W/D relationship and inversion has to be performed on this curve only. Thanks to the scaling properties of SWs (Socco and Boiero, 2008; Maraschini et al. 2011), models with the same velocity contrasts but with different velocity ranges will provide the same W/D relationship. Therefore, the W/D relationship obtained for one curve will perfectly predict the V_{Sz} of scaled models. The choice of a proper DC as reference should then be based on the analysis of the shape rather than the average velocity value.

The synthetic data present a higher lateral variability than the expected lateral variability in the two field cases. However, for field case 2, because two sets of DCs with clearly different trends are identified, the data set has been split in two. For the field data, we have used as a benchmark the results of laterally constrained and joint inversion of the DCs, respectively, and we have also compared the results with DHTs. We have tested the method with high-quality data from areas with smooth velocity gradients (field case 1)

and with poor-quality data from areas with velocity inversions and contrasts (field case 2). For both sites, the estimated V_{Sz} has errors mostly less than 5% (Figures 9c and 11c).

The synthetic and field examples show that the errors in the estimation of V_{Sz} tend to be larger at shallow depths, whereas the estimate is more reliable and stable at greater depths (Figures 5a and 7a). This is due to the lack of data points and poor resolution in the first few meters from the ground surface. In fact, because the method is based on a data transform, the quality of the estimation depends on the quality of the DC and on the availability of data points at different wavelengths. This can also be seen on the results of field data in which the higher errors are in the zones of poor data coverage, particularly in the very shallow subsurface (Figures 9c and 11c). All the synthetic results underline, however, that the error reduces and remains stable with increasing depth, particularly below the bedrock. This leads to reliable estimates of the one-way time below the bedrock for statics.

In Figure 12, we show the error distributions on one-way time in milliseconds for the two synthetic data sets. We use box plots with the same scheme used for Figures 5b and 7b, and we report the distribution of errors of all the profiles at all depths obtained using different reference models to estimate the W/D. Most of the values fall within 5 ms except for few outliers and a couple of cases already evidenced in the normalized error for the velocities (Figures 5b and 7b).

In Figures 9d and 11d, we compare the static shift computed from the velocity models obtained through inversion and those obtained from the direct estimation and showed that the spatial trends are very well-reconstructed. In Figure 13, we report the distribution of the time differences in Figures 9d and 11d in the form of histograms. In both situations, the difference with respect to the inversion results remains less than 5 ms except for a few outliers. The distribution of the one-way traveltime differences is centered at zero for field case 1, and it shows a very slight global overestimation for field case 2. In this respect, it is useful to remark that the two benchmarks used are different from each other. In field case 1, LCI was performed with a vertical smoothness constraint and a high number of layers; hence, the resulting models are vertically smooth. In field case 2, on the contrary, joint inversion was performed using a limited number of layers that led to higher contrast within the benchmark velocity models. Moreover, comparing the one-way time obtained with our approach with the available traveltimes obtained directly from borehole data (Figure 11d), it can be noted that our estimate is in better agreement with the DHTs and that both are slightly higher than the time obtained from LCI, particularly in the south zone.

The field data confirm the possibility of replicating the results of the inversion in terms of V_{Sz}, without the need of inverting the whole data set. Removing extensive inversion from the workflow reduces the need for arbitrary choices from the operator (model parameterization) and avoids a possible source of error. Moreover, it makes the process very fast. The fact that the results are mainly data driven makes the uncertainty in the results directly related to data coverage and experimental uncertainties. It is hence of paramount importance to assess that the DCs obtained from the seismic records guarantee the sufficient investigation depth and lateral resolution. The possibility of extracting broadband and high-quality DC depends on acquisition parameters and on site characteristics. If the DCs are retrieved from seismic reflection records acquired for hydrocarbon exploration, countermeasures taken to filter ground roll during acquisition, such as geophone groups or high-pass filters, can affect the data quality. A practical guideline for the acquisition parameters can be found in Socco et al. (2010), and a discussion about the extraction of dispersion data from hydrocarbon exploration seismic records is provided in Strobbia et al. (2011). As far as our experi-

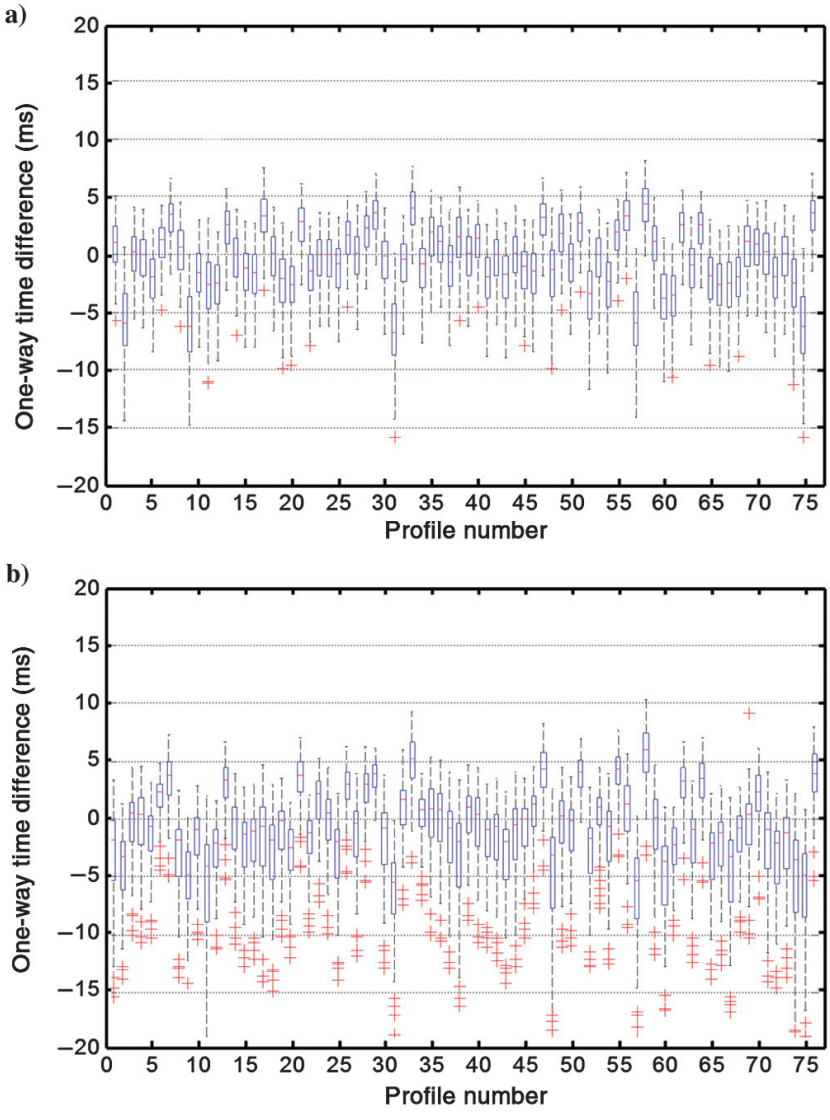

Figure 12. Box plots of the mean one-way time error for the two synthetic data sets using different reference profiles (and different W/D relationships): (a) synthetic data set 1 and (b) synthetic data set 2.

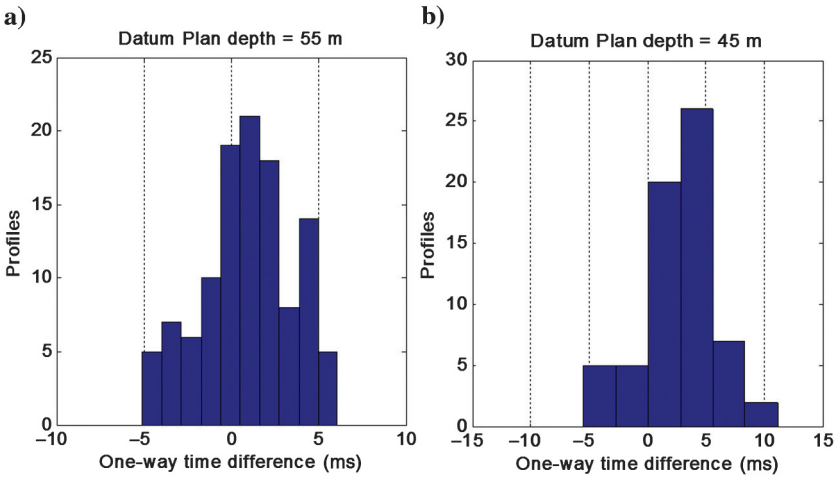

Figure 13. One-way time difference of the proposed approach with respect to the benchmark inversions for field cases (a) 1 and (b) 2.

ence is concerned, vibroseis sources provide broadband data that allow significant investigation depth, often of some hundreds of meters. The most critical aspect of the acquisition layout of exploration data is usually the coarse sensor spacing, which can produce spatial aliasing. An example of processing workflow to optimize the quality of DCs obtained from 2D seismic reflection records is presented in Socco et al. (2009), where lateral resolution is also discussed. According to the obtained investigation depth, this method can be considered as an alternative or as complementary to other near-surface investigation techniques usually applied to estimate the velocity of the weathering layer (e.g., up-holes and high-resolution seismic surveys). In particular, the investigation depth is related to the maximum retrieved wavelength: If this is larger than the datum depth, this method can substitute other techniques, if it is shorter than the datum depth, complementary measurements are required.

The field examples presented in this work are 2D, but the method can be directly applied to 3D data. Each DC is in fact associated with a local 1D model; hence, there is no difference if the 1D models are distributed along a line or over an area. The extraction of DC from 3D data can be performed with techniques similar to those applied to 2D data and provides a set of local DCs distributed over the investigated area (see e.g., Boiero et al., 2011; Strobbia et al., 2011). Hence, the method we propose is locally 1D and can be applied to retrieve 2D or 3D distribution of the near-surface S-wave velocity.

CONCLUSION

Our work shows that it is possible to estimate the time-average velocity along a seismic line directly from the SW DCs, given the knowledge of one V_S model corresponding to one of the DCs. This is done by computing the W/D relationship for the known model and then using it to estimate the time-average velocity corresponding to all the other DCs.

Our approach has been proven to be effective on sites with lateral variations in near-surface velocities on synthetic and field data. The results show that the time-average velocity can be estimated with uncertainty of the order of 10% for highly laterally variable synthetic data and approximately 5% on field data with smooth lateral variations. Uncertainties on one-way time (static shift) are mostly within 5 ms for synthetic and real data. This novel method is strongly data dependent, and, hence, the quality of the estimate strongly depends on the data uncertainty and coverage. This requires careful processing to extract DCs and broadband seismic data to guarantee the sufficient investigation depth.

The method offers a novel possibility to directly estimate static corrections for V_S using the groundroll present in seismic data, with no need for massive inversion of the DCs. Besides computation of V_S statics for seismic exploration processing, the presented approach also appears attractive in seismic hazard studies when a large number of sites need to be classified through $V_{S,30}$. In this case, the W/D relationship could be estimated for an area and then the $V_{S,30}$ can be directly obtained by the local DCs of different sites. Moreover, the 2D V_{Sz} profiles obtained for the two field cases suggest that the proposed data transformation can be used for the construction of reliable initial models to be used in more sophisticated full-waveform inversions approaches and provide near-surface velocity models to be included in other seismic processing steps.

A natural extension of this method is the analysis of the sensitivity of the W/D relationship to Poisson's ratio. This is analyzed in a companion paper Socco and Comina (2017). A further extension would be to include higher modes of SW propagation in the analyses.

ACKNOWLEDGMENTS

The Seismic Service of the Environment Regional Agency of the Piemonte Region (ARPA Piemonte) and the Natural Risk Management and Observational Seismology Department of the Aosta Valley Region supported the data acquisition and allowed publication of the data of the two field examples. The EU-financed Interreg III B — Alpinespace — Sismovalp project "Seismic hazard and alpine valley response analysis" through which the field data were acquired.

REFERENCES

Al Dulaijan, K., and R. R. Stewart, 2010, Using surface-wave methods for static corrections: A near-surface study at Spring Coulee, Alberta: 80th Annual International Meeting, SEG, Expanded Abstracts, 1897–1901.

Auken, E., and A. V. Christiansen, 2004, Layered and laterally constrained 2D inversion of resistivity data: Geophysics, **69**, 752–761, doi: 10.1190/1.1759461.

Aung, A. M. W., and E. C. Leong, 2015, Application of weighted average velocity (WAVe) method to determine $V_{S,30}$: Soils and Foundations, **55**, 548–558, doi: 10.1016/j.sandf.2015.04.007.

Boiero, D., P. Bergamo, R. B. Rege, and L. V. Socco, 2011, Estimating surface wave dispersion curves from 3D-seismic acquisition schemes: Part 1 — 1D models: Geophysics, **76**, no. 6, G85–G93, doi: 10.1190/geo2011-0124.1.

Boiero, D., P. Marsden, V. Esaulov, A. Zarkhidze, and P. Vermeer, 2013, Building a near-surface velocity model in the South Ghadames Basin: Surface-wave inversion to solve complex statics: 83rd Annual International Meeting, SEG, Expanded Abstracts, 1811–1815.

Boiero, D., and L. V. Socco, 2011, The meaning of surface wave dispersion curves in weakly laterally varying structures: Near Surface Geophysics, **9**, 561–570, doi: 10.3997/1873-0604.2011042.

Boiero, D., and L. V. Socco, 2014, Joint inversion of Rayleigh-wave dispersion and P-wave refraction data for laterally varying layered models: Geophysics, **79**, no. 4, EN49–EN59, doi: 10.1190/geo2013-0212.1.

Brown, L. T., J. G. Diehl, and R. L. Nigbor, 2000, A simplified procedure to measure average shear-wave velocity to a depth of 30 meters ($V_{S,30}$): Presented at the 12th World Conference on Earthquake Engineering.

Comina, C., S. Foti, D. Boiero, and L. V. Socco, 2011, Reliability of $V_{S,30}$ evaluation from surface waves tests: Journal of Geotechnical and Geoenvironmental Engineering, **137**, 579–586, doi: 10.1061/(ASCE)GT.1943-5606.0000452.

Douma, H., and M. Haney, 2011, Surface-wave inversion for near-surface shear-wave velocity estimation at Coronation field: 81st Annual International Meeting, SEG, Expanded Abstracts, 1411–1415.

Dunkin, J., 1965, Computation of modal solutions in layered, elastic media at high frequencies: Bulletin of Seismological Society of America, **55**, 335–358.

Ernst, F., 2007, Long-wavelength statics estimation from guided waves: 69th Annual International Conference and Exhibition, EAGE, Extended Abstracts, E033.

Haney, M., and R. Miller, 2013, Introduction to this special section: Non reflection seismic and inversion of surface waves and guided waves: The Leading Edge, **32**, 610–611, doi: 10.1190/tle32060610.1.

Haney, M. M., and V. C. Tsai, 2015, Non perturbational surface-wave inversion: A Dix-type relation for surface waves: Geophysics, **80**, no. 6, EN167–EN177, doi: 10.1190/geo2014-0612.1.

Haskell, N., 1953, The dispersion of surface waves on multilayered media: Bulletin of the Seismological Society of America, **43**, 17–34.

Herrmann, R. B., and C. J. Ammon, 2002, Computer programs in seismology: Surface waves, receiver functions and crustal structure, version 3.20: Saint Louis University.

Khosro Anjom, F., 2016, Direct estimation of S-wave velocity from ground-roll (Rayleigh waves) towards static corrections: M.S. thesis, Politecnico di Torino.

Leong, E. C., and A. M. W. Aung, 2012, Weighted average velocity forward modelling of Rayleigh surface waves: Soil Dynamics and Earthquake Engineering, **43**, 218–228, doi: 10.1016/j.soildyn.2012.07.030.

Mabyalaht, G. S., 2015, Consequences of surface wave non uniqueness on static corrections: M.S. thesis, Politecnico di Torino.

Maraschini, M., 2008, A new approach for the inversion of Rayleigh and Scholte waves in site characterization: Ph.D. dissertation, Politecnico di Torino.

Maraschini, M., D. Boiero, S. Foti, and L. V. Socco, 2011, Scale properties of the seismic wavefield: Perspectives for full waveform matching: Geophysics, **76**, no. 5, A37–A44, doi: 10.1190/geo2010-0213.1.

Roy, R., R. R. Stewart, and K. Al Dulaijan, 2010, S-wave velocity and statics from ground-roll inversion: The Leading Edge, **29**, 1250–1257, doi: 10.1190/1.3496915.

Socco, L. V., and D. Boiero, 2008, Improved Monte Carlo inversion of surface wave data: Geophysical Prospecting, **56**, 357–371, doi: 10.1111/j.1365-2478.2007.00678.x.

Socco, L. V., D. Boiero, C. Comina, S. Foti, and R. Wisén, 2008, Seismic characterization of an Alpine Site: Near Surface Geophysics, **6**, 255–267, doi: 10.3997/1873-0604.2008020.

Socco, L. V., D. Boiero, S. Foti, and R. Wisén, 2009, Laterally constrained inversion of ground roll from seismic reflection records: Geophysics, **74**, no. 6, G35–G45, doi: 10.1190/1.3223636.

Socco, L. V., and C. Comina, 2015, Approximate direct estimate of S-wave velocity model from surface wave dispersion curves: 21st Annual International Conference and Exhibition, EAGE, Extended Abstracts, A09.

Socco, L. V., and C. Comina, 2017, Time-average velocity estimation through surface-wave analysis: Part 2: P-wave velocity: Geophysics, **82**, this issue, doi: 10.1190/geo2016-0368.1.

Socco, L. V., S. Foti, and D. Boiero, 2010, Surface wave analysis for building near surface velocity models: Established approaches and new perspectives: Geophysics, **75**, no. 5, 75A83–75A102, doi: 10.1190/1.3479491.

Socco, L. V., G. Mabyalaht, and C. Comina, 2015, Robust static estimation from surface wave data: 85th Annual International Meeting, SEG, Expanded Abstracts, 5222–5227.

Strobbia, C., A. Laake, P. Vermeer, and A. Glushchenko, 2011, Surface waves: Use them then lose them. Surface-wave analysis, inversion and attenuation in land reflection seismic surveying: Near Surface Geophysics, **9**, 503–513, doi: 10.3997/1873-0604.2011022.

Thomson, W. T., 1950, Transmission of elastic waves through a stratified solid medium: Journal of Applied Physics, **21**, 89–93, doi: 10.1063/1.1699629.